CHAPTER IV
MODIFICATION OF POROUS CLAY HETEROSTRUCTURES (PCHs) AND MAGNETIC POROUS CLAY HETEROSTRUCTURES (MAGNETIC PCHs)

4.1 Abstract

Porous clay heterostructures (PCHs) are a recent class of solid porous materials, where the PCH surface areas are higher than oraganoclay. In this work, a PCH surface was modified by Fe ion (Fe^{2+} and Fe^{3+}), from the ferric chloride hexahydrate for using as magnetic sensor. To investigate the effect of the molar ratio of dodecylamine/TEOS on the formation of porous structures, the products were characterized by N_2 adsorption-desorption, XRD, SEM, TEM and FTIR techniques. The results reveal that PCHs had surface areas of 412–688 m^2/g, average pore diameter in the range of 4.06–7.86 nm, and pore volume of 0.70–0.83 cc/g, respectively while Magnetic PCHs had a result of 148–170 m^2/g, average pore diameter in the range of 12.17–14.58 nm, and pore volume of 0.51–0.66 cc/g, respectively. The results of UV/vis absorbance spectra showed that the absorbance spectra of PCH, magnetic PCH (5-20%wt of Fe ion) and bentonite had the appearance of a broad band at 242 nm points to the charge transportation from O^{2-}, OH^-, or H_2O to the iron (Fe^{3+}) in the octahedral layer of the clay mineral. From SEM images and consistent EDX micrograph of Fe ion in PCH, the results showed that the incorporation of Fe ion in PCH was successful. Magnetic PCH exhibited a remarkably significant bacteriostatic effect against *Escherichia coli* and *Staphylococcus aureus*.

keywords : Porous clay heterostructures (PCH), Co-surfactant template, Bentonite

4.2 Introduction

Recently, the discovery of a new class of porous materials known as porous clay heterostructures (PCHs) has been proposed [1]. This porous material is prepared by surfactant-directed assembly of silica in the two dimensional interlayer spacing of clays [2-6]. The PCHs materials reveal important properties such as exhibiting high surface areas with uniform and specific pore sizes in the rarely observed

supermicropore to small mesopore region [6]. In the synthesis of PCHs, layered clays are first intercalated with cationic surfactants. Neutral amine co-surfactant molecules are then intercalated along with silica species which leads to the polymerization of siloxane network surrounding the surfactant micelles in the clay galleries. Then, an open-framework of silica is formed in the galleries after surfactant removal [7]. From this viewpoint, these porous materials could find application in many fields. The PCH surface area is higher than oraganoclay, making it suitable for easily modified by functional group and higher surface area for scavenging system. The previous work [8] showed the dramatically enhanced surface area of PCH compared to bentonite and successfully attached the surface of PCH with methyl group. These modified PCH exhibited the increasing of ethylene adsorption. The continuous work [9] involved the modification of PCH's surface by thiol group to enhance the conductive properties of these PCHs.

This work was focused on another point of view; to enhance the magnetic properties of PCH surface for using as magnetic sensor filler in film packaging. The molar ratio of dodecylamine/TEOS and then study components in clay. The magnetic properties of mesoporous was modified by $Fe^{2+}$and Fe^{3+} ions by adding the ferric chloride hexahydrate and testing methods to evaluate the anti-bacterial performance. Subsequently, these as-synthesized mesoporous materials were blended with polylactide, and the properties concerning the capability of polylactide-magnetic PCHs nanocomposites in food packaging and magnetic sensor were investigated.

4.3 Experimental

Materials

Na-Bentonite (BTN), (Mac-Gel® GRADE SAC), was obtained from Thai Nippon Chemical Industry Co., Ltd. The cation exchange capacity (CEC) of BTN is 55 mmol/100g of clay.

Cetyltrimethylammonium $[C_{16}H_{33}N^{+}(CH_3)_3]$ bromide (CTAB) was supplied by Fluka. Dodecylamine, $C_{12}H_{27}N$, (MW=185.35), (98% purified) was supplied by Aldrich. Tetraehtyl orthosilicate (TEOS), (MW=208.33), Ammonium hydroxide

(NH_4OH) and Ferric chloride hexahydrate ($FeCl_3.6H_2O$) were purchased from Fluka. Methanol (CH_3OH) was supplied by Lab Scan and Hydrochoric acid (HCl) was supplied by Carlo Erba. Polylactide 4042D (PLA) was supplied by NatureWorks Co., Ltd and Polycaprolactone was supplied by Aldrich.

Purification and pH Adjustment of Bentonite

Bentonite was pulverized and sieve through 325 mesh. Four 10-g of the passing part were purified by centrifugation and then washed with distilled water several time until pH value was near 7. After that, centrifugation was applied. Again, the same amount of distilled was added, and then the sample was adjusted to pH 9.0 by using dilute HCl and NaOH solutions. The samples were air-dried overnight and pulverized in a mortar.

Synthesis of Porous Clay Heterostructures (PCHs)

The bentonite was converted into a quaternary ammonium exchange form by ion exchange with cetyltrimethylammonium bromide and stirred at 50°C for 24 h. After the reaction time, the solid was filtered out, washed with a mixture of methanol and water and then air-dried. The obtained organoclay was stirred in dodecylamine for 30 min at 50°C following which TEOS was added and study the molar ratio of dodecylamine/TEOS for clay 1 g. The resulting suspension was stirred for further 4 h at room temperature. The solid was separated from solution by filtration and air-dried overnight at room temperature to form the as-synthesized PCH. The surfactant was removed from the as-synthesized PCH using methanol/HCL solution. Typically, 1 g of the as-synthesized PCH material has been added to 45 mL of methanol and 5 mL of HCl and refluxed for 2 h. The solid was subsequently filtrated out mixture of methanol and water and air-dried at room temperature overnight to obtain PCHs.

Preparation of Magnetic PCHs

Ferric chloride hexahydrate was used as iron sources which it was added in PCH at 0,5,10,15,20 wt%. Aqueous ammonia was used as the precipitator. Distilled water was used as the solvent. Before the reaction, N_2 gas was flown through the

reaction medium. The reaction was operated in a closed system to provide a nonoxidation environment. NH_4OH was slowly injected into PCH which added ferric chloride hexahydrate under stirring 30 min. The dispersion was centrifuged at 3000 rpm for 20 min. After precipitation, the Fe_3O_4 particles in PCH were repeatedly washed and filtered before drying at room temperature in air atmosphere to form powders.

Physical Measurements

Powder X-ray diffraction patterns were measured on a Rigaku Model Dmax 2002 diffractometer with Ni-filtered Cu K_α radiation operated at 40 kV and 30 mA. The powder samples were observed on the 2θ range of 2-20 degree with a scan speed of 2 degree/min and a scan step of 0.02 degree.

N_2 adsorption-desorption isotherms were obtained at -196°C on a Quantachrome Autosorb-1. Powder samples were degassed at 150°C during 12 h under vacuum prior to analysis. Surface areas were calculated using the BET equation. The pore size distributions were constructed based on Barrett, Joyner and Halenda (BJH) method using the adsorption branch of the nitrogen isotherm.

Scanning electron microscopy was performed on JSM-6400 Model. The specimens were coated with gold under vacuum to make them electrically conductive.

Transmission electron microscopy was performed on JEOL JEM-2100 model and an accelerating voltage of 150 kV. TEM samples were prepared by embedding the powder in resin and sectioning on a ultramicrotome.

Gas chromatography (Agilent Technologies 6890 Network GC system) and HP-PLOT Q column: 30 m x 0.32 mm ID with flame ionization detector was utilized to examine ethylene adsorption capacity of the porous clays. Helium gas was used as carrier gas and the initial temperature for injection step was 150°C. Ethylene adsorption was measured by placing each product in a jar (0.6 l), then sealing with a screw-cap lid. Ethylene was injected into a jar to give a specific concentration of 500 ppm. Ethylene concentration in the jar was measured periodically about once an

hour. The ethylene adsorption was calculated by taking the difference between the amount of ethylene added and the amount of remaining in the headspace.

UV/VIS Spectrophotometer was recorded on a UV/vis spectrophotometer 2550 (Shimadzu) scanning in the range of 200-1000 nm at room temperature. Experiments were performed in a solid stub.

Antimicrobial Activity Testing was used to observe antibacteria efficiency that was performed in Luria–Bertani (LB) medium solid agar Petri dish. Starting to inoculate *Escherichia coli* and *Staphylococcus aureus* bacteria into growth medium. Approximately 10^7 colony-forming units (CFU) of each microorganism was spread on agar plates. After that, the PCH containing Fe ion was sterilized by autoclaving 15 min at 120°C and then placed on *Escherichia coli*-cultured and *Staphylococcus aureus*-cultured agar plates, which will be then incubated for 24 h at 37°C. The zone of inhibition was then measured clear zone and recorded.

Chemical Analysis

FT-IR spectra of organoclay, PCHs, and magnetic PCHs were obtained using a Nicolet Nexus 670 FT-IR spectrometer in the frequency range of 4000-400 cm^{-1} with 32 scans at a resolution of 2 cm^{-1}. KBr pellet technique was applied in the preparation of powder samples. The incorporation of organic group into silicate network was investigated by using FTIR technique.

4.4 Results and Discussion

Effect of molar ratio of surfactants to pore characteristic

Table 4.1 shows the results of N_2 adsorption. The BET surface area of BTN was 53 m^2/g while the surface areas of PCHs increased significantly from pristine clay. The results showed that PCHs had surface areas of 412–688 m^2/g, average pore diameter in the range of 4.06–7.86 nm, and pore volume of 0.70–0.83 cc/g, respectively. The isotherm of BTN belongs to type II characteristic of nitrogen adsorption on macroporous adsorbents (Figure 4.1). The isotherms of PCHs are shown in Figure 4.1 which were abruptly increased in nitrogen adsorption at low partial pressure and gradually increased to medium partial pressure (P/P_0:0.05–0.3) suggested that these materials possess supermicropore to small mesopore region, belong to type IV, corresponding to mesoporous adsorbents.

From the results in Table 4.1, The PCH obtained by the molar ratio of dodecylamine and TEOS: 20/200 (D/T = 20/200) was suitable to modify their surfaces with magnetic functional group because of the high pore volume and the high surface area.

Table 4.1 Porosity characteristics of BTN and PCHs

Sample	Multipoint BET surface area (m^2/g)	Average pore diameter (nm)	BJH pore volume (cc/g)
Bentonite	53	9.64	0.17
PCH (D/T = 20/50)	688	4.06	0.70
PCH (D/T = 20/100)	545	5.65	0.77
PCH (D/T = 20/150)	412	7.68	0.80
PCH (D/T = 20/200)	609	5.35	0.82
PCH (D/T = 20/250)	438	7.60	0.83

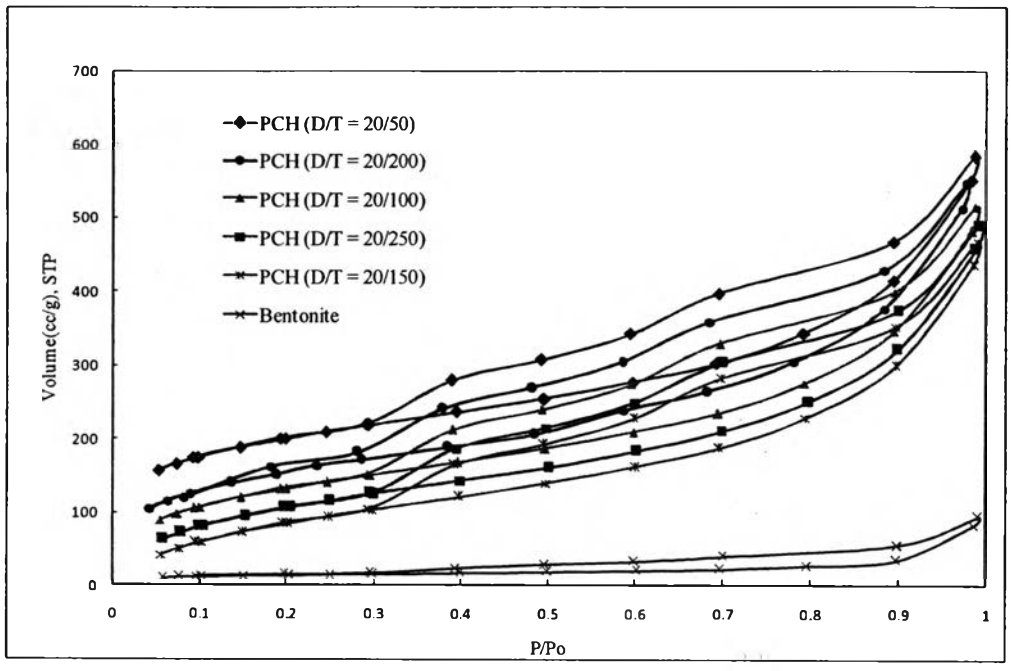

Figure 4.1 N_2 adsorption-desorption isotherms of bentonite and PCHs.

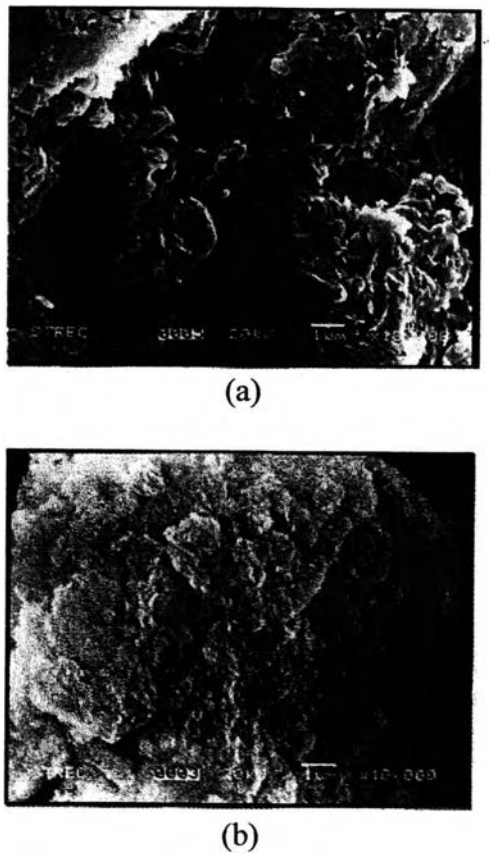

(a)

(b)

Figure 4.2 SEM images of (a) BTN and (b) PCH (D/T = 20/200).

For the surface morphology, the BTN exhibited a layered or plate-like structure in SEM image as shown in Figure 4.2(a). After modification, the SEM image of PCH in Figure 4.2(b) reveal a similar morphology to starting clay but more surface rougher than that of BTN. According to N_2 adsorption-desorption results in Figure 4.1 and Table 4.1, the surface areas of PCHs increased significantly compared to those of pristine clay.

Effect of the Molar Ratio of Dodecylamine and TEOS on the Interlayer Distance of PCHs

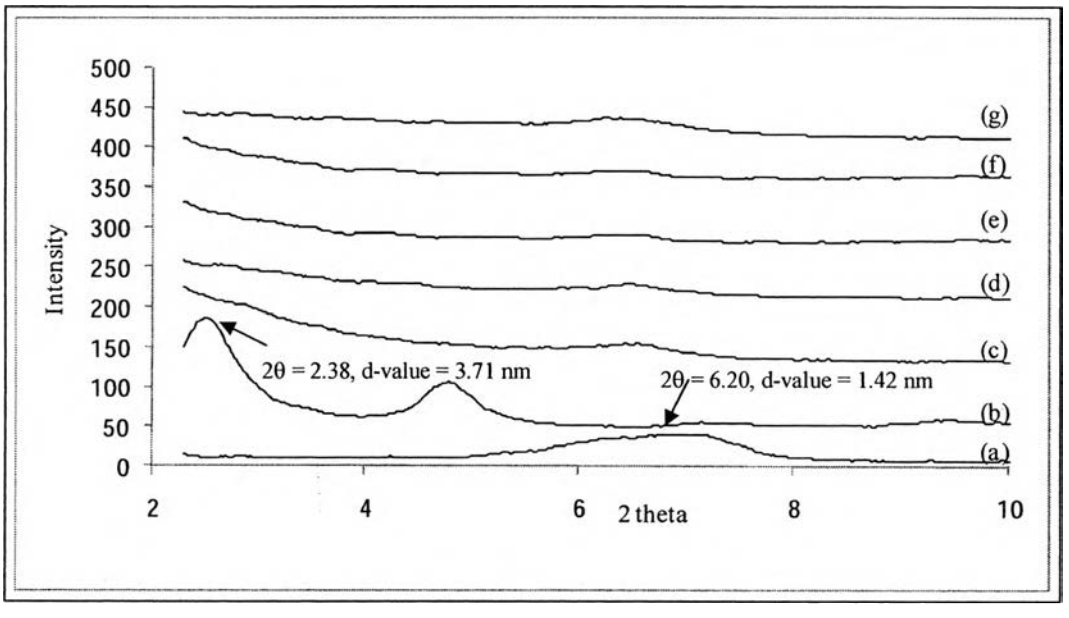

Figure 4.3 The XRD patterns of : (a) BTN, (b) Organoclay, (c) PCH (D/T = 20/50), (d) PCH (D/T = 20/100), (e) PCH (D/T = 20/150), (f) PCH (D/T = 20/200), (g) PCH (D/T = 20/250).

Table 4.2 The basal spacing of BTN and organoclay

Sample	2θ (degree)	d-value (nm)
BTN	6.20	1.42
Organoclay	2.38	3.71

A corresponding XRD pattern of the samples are shown in Figure 4.3(a) and Table 4.2, the basal spacing of BTN is 1.42 nm and show the presence of the (001) reflection peak. After BTN was treated with cetyltrimethylammonium bromide (CTAB) to obtain organoclay, the peak of starting clay at $2\theta = 6.20°$ ($d = 1.42$ nm) disappeared (Figure 4.3(b)), two strong peaks were observed at lower angle as a consequence of the successful intercalation of cationic surfactant in the interlayer of BTN, resulting in the increasing of distance between clay layers. The results are shown in Table 4.2.

The clay galleries were first opened up by the intercalation of the surfactant cetyltrimethylammonium cation. Subsequently, neutral amine co-surfactant was then intercalated between clay layers to form micelle templates. Then silica sources (TEOS) was introduced to polymerize surrounding the surfactant micelles in the galleries of clay. By solvent extraction method, the surfactant templates were removed from as-synthesized PCHs, resulting in the formation of porous structures.

The XRD patterns of these samples are illustrated in Figure 4.3(c)-(g). There was no obvious peak observed in the XRD patterns of PCHs. A possible reason might be due to the disordered structure of silica framework which was formed in the galleries of clay shielding a highly regular interstratification of the clay layers.

Characterization of Magnetic PCHs

Table 4.3 shows the results of N_2 adsorption. The BET surface area of PCH was 609 m^2/g while the surface areas of magnetic PCHs decrease significantly from PCH. The results showed that Magnetic PCH had surface areas of 148–170 m^2/g, average pore diameter in the range of 12.17–14.58 nm, and pore volume of 0.51–

0.66 cc/g, respectively. The isotherms of magnetic PCH are shown in Figure 4.3 belong to type IV, corresponding to mesoporous adsorbents.

Magnetic PCHs exhibited a high average pore diameter and a less surface area as compared with the PCHs (Table 4.1 and 4.3) because the pore structures were collapsed and the Fe ion can aggregate by the hydrolysis of iron salts.

Table 4.3 Porosity characteristics of PCH and Magnetic PCH

Sample	Multipoint BET surface area (m^2/g)	Average pore diameter (nm)	BJH pore volume (cc/g)
PCH (D/T = 20/200)	609	5.35	0.82
Magnetic PCH (Fe 5%)	152	13.54	0.51
Magnetic PCH (Fe 10%)	170	12.17	0.66
Magnetic PCH (Fe 15%)	164	12.18	0.65
Magnetic PCH (Fe 20%)	148	14.58	0.54

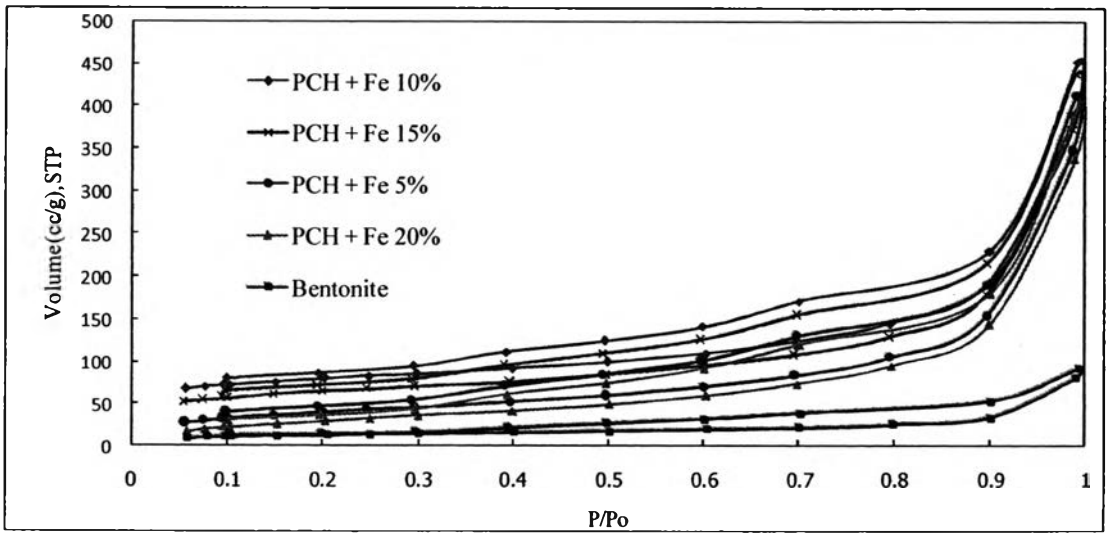

Figure 4.4 N_2 adsorption-desorption isotherms of BTN and Magnetic PCH .

In the TEM image provided in Figure 4.5, the clay layers were discernible as solid dark lines which were easily observed. The framework pore orientation was not persistent. However, the presence of the dispersion on the clay layers in Figure 4.5(b), the Fe particles were discernible as dark spots and It can be seen that the iron co-aggregates.

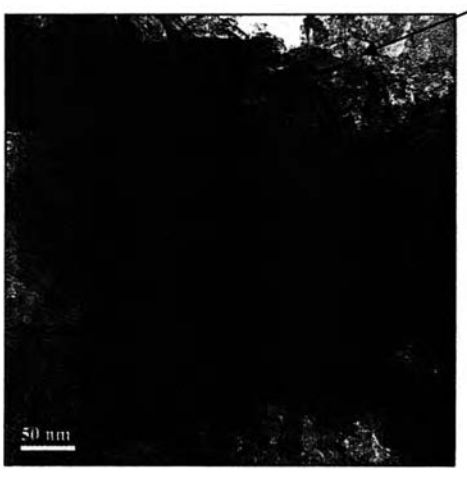

(a)

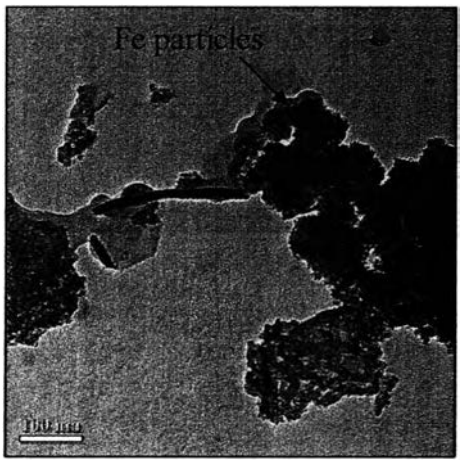

(b)

Figure 4.5 TEM image of (a) magnetic PCH (Fe 20%) and (b) magnetic PCH (Fe 20%) (zoom out).

The FTIR spectrum of BTN is given in Figure 4.6(a). The broad peak around 3500 cm^{-1} can be assigned to the stretching vibration of the silanol associated with the silica structure. The peak at 1000, 1100 and 800 cm^{-1} can be assigned to the

stretching vibration of the SiO_4 units, the asymmetric and symmetric stretching vibrations of the Si-O-Si linkage, respectively. The presence of surfactant was evidenced by FTIR spectra of organoclay (Figure 4.6(b)) indicating the asymmetric and symmetric vibrations of methyl and methylene groups of cetylrimethyl ammonium ion at 2920 and 2985 cm^{-1}, respectively. The FTIR spectra of PCH (D/T = 20/200) (Figure 4.5(c)) was different from starting BTN indicated by the absence of peak at 1000 cm^{-1}. So it roughly infers that the structure of starting clay was changed after the modification. Moreover, the spectra of magnetic PCH (Figure 4.6(d)) reveal a similar spectra to PCH(D/T = 20/200).

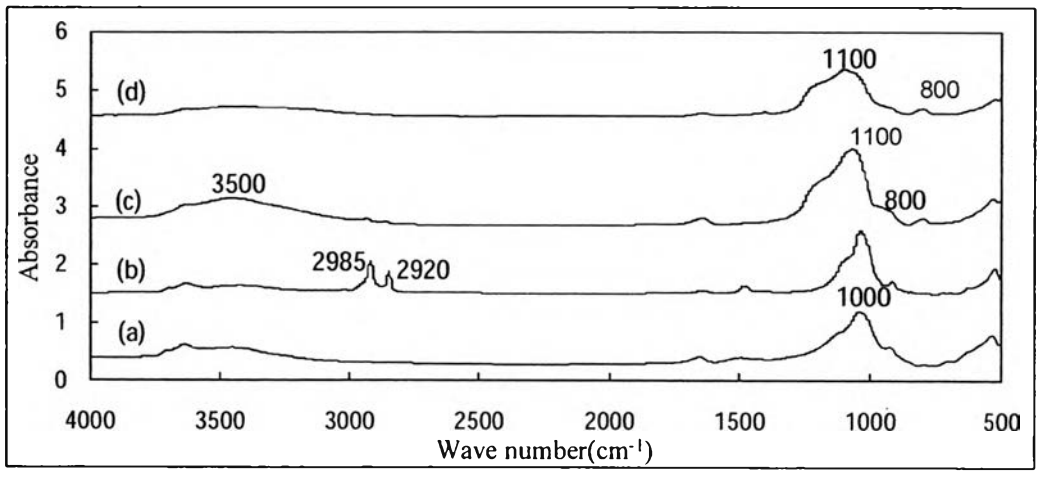

Figure 4.6 FTIR spectra of (a) BTN, (b) organoclay, (c) as-synthesized PCH and (d) magnetic PCH (Fe20%).

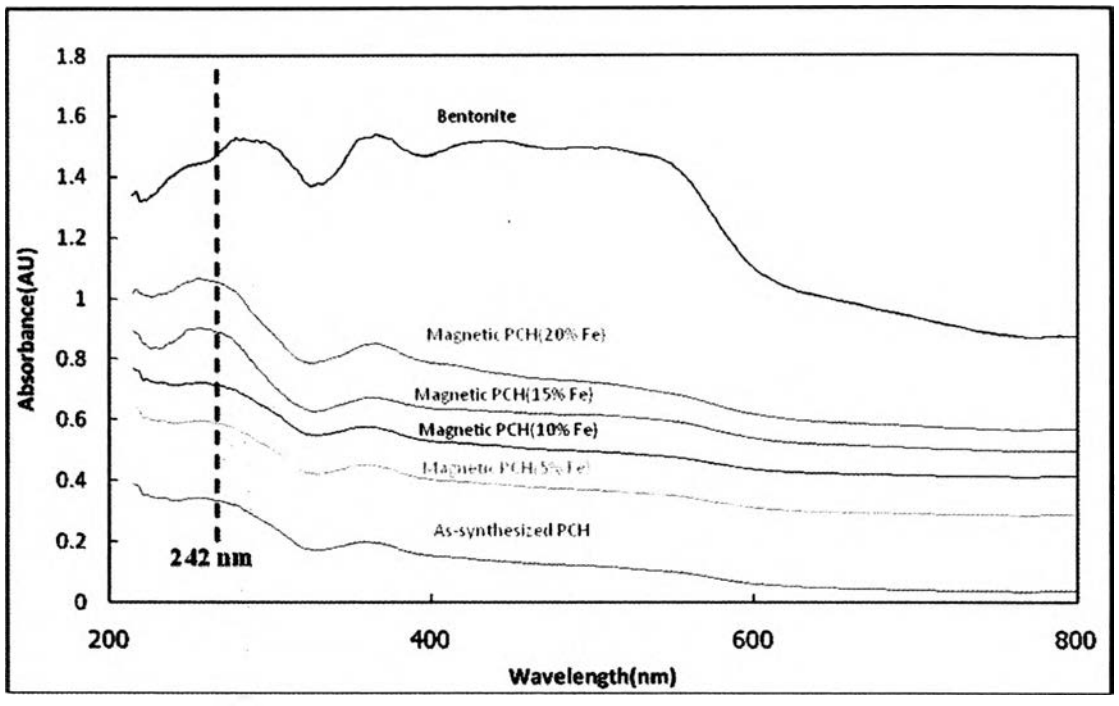

Figure 4.7 UV/vis absorbance spectra of as-synthesized PCH, magnetic PCHs and BTN.

In addition, to ensure the existence of ferric ion in the octahedral sheet, UV/vis spectrophotometry was carried out as well. The basic structural SiO_4 units of tetrahedral sheets in the clay lattice do not absorb light in the wavelength ranging from 200 to 800 nm, except when the transition metal ions in the silicate structure are exchanged. Transition metal cations (e.g. Fe^{3+} and Al^{3+}) appearing at both the crystal edges and the planar surfaces of smectite clay can act as an oxidizing agent (electron acceptor). Figure 4.7 shows the absorbance spectra of PCH, magnetic PCH (Fe 5-20%) and BTN, the appearance of a broad band at 242 nm points to the charge transportation from O^{2-}, OH^-, or H_2O to the iron (Fe^{3+}) in the octahedral layer of the clay mineral.

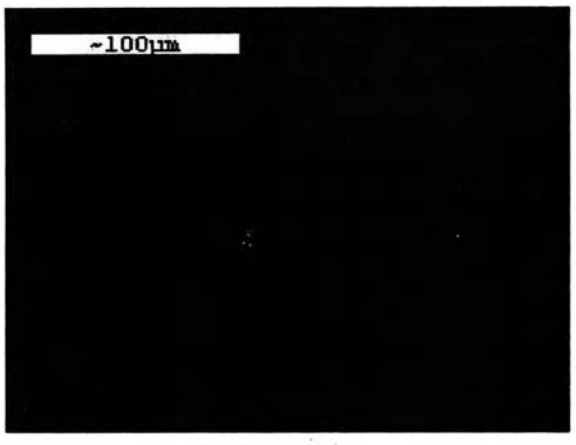

(a)

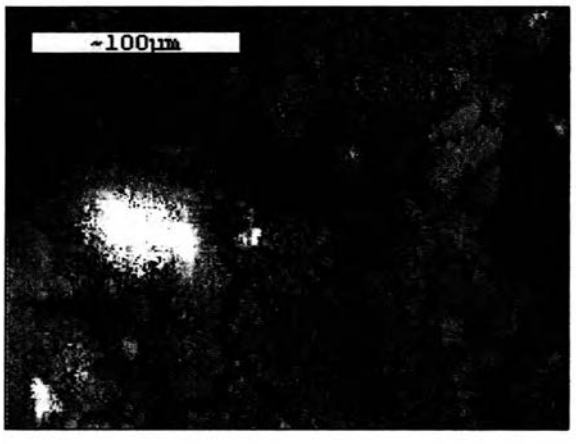

(b)

Figure 4.8 SEM image and consistent EDX micrograph of 5%wt Fe ion in PCH (a) Fe mapping, (b) SEM image.

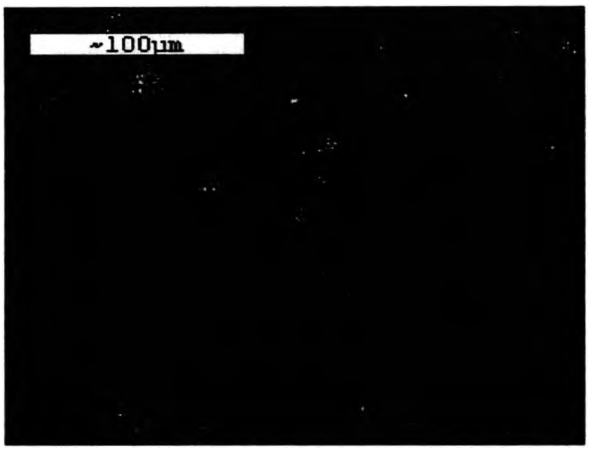

(a)

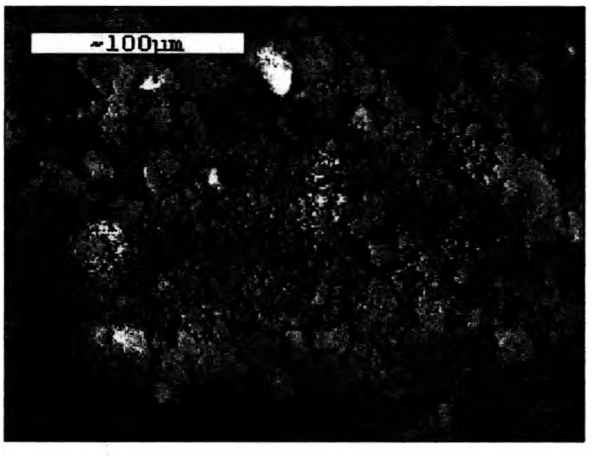

(b)

Figure 4.9 SEM image and consistent EDX micrograph of 20 %wt Fe ion in PCH (a) Fe mapping, (b) SEM image.

The preliminary results of Fe attachment on PCH surface was successfully observed by EDX micrographs in Figures 4.8 and 4.9. As increasing the percentage of ferric chloride hexahydrate in PCH, the EDX mappings show the higher content of Fe ion in PCH.

Antimicrobial Activity Testing

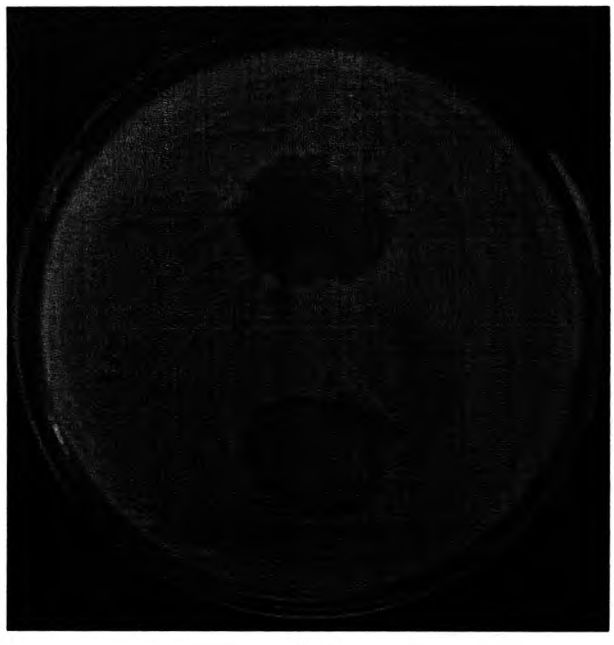

(a)

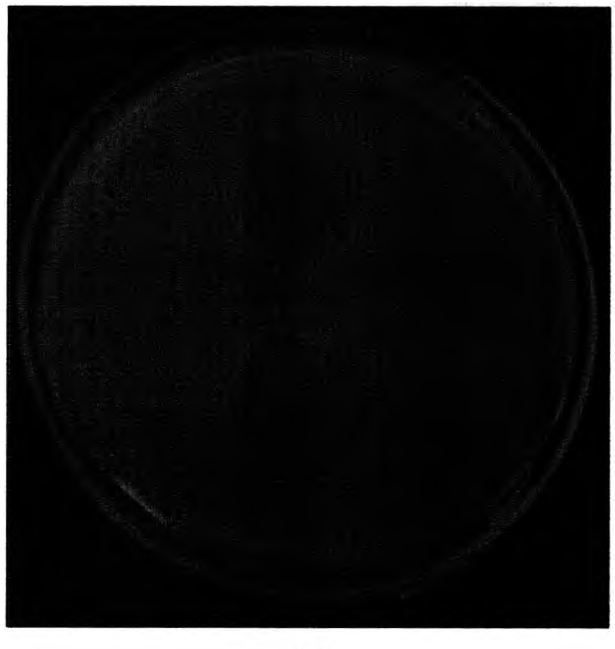

(b)

Figure 4.10 Images of Antibacteria (upper : PCH(D/T = 20/200), lower : magnetic PCH(Fe 20%)) ; (a) *Escherichia coli*, (b) *Staphylococcus aureus*.

PCH(D/T = 20/200) was marginally active against *Escherichia coli*, as observed from Figure 4.10 which could generate zones of inhibition of 15 mm on the Petri dishes and were inactive against *Staphylococcus aureus*. Magnetic PCH (20% Fe) exhibited a remarkably significant bacteriostatic effect against *Escherichia coli* and *Staphylococcus aureus* which generated zones of inhibition of 25 mm and 20 mm, respectively. This also indicates that magnetic PCH (Fe 20%) was diffusible and could perform an inhibition of the bacteria growth. The clear zone was clearly visible for magnetic PCH.

Table 4.4 Inhibition zones of bacteria on PCH and magnetic PCH

Type of Clay	Zones of inhibition (nm)	
	Escherichia coli	*Staphylococcus aureus*
PCH (D/T = 20/200)	15	inactive
Magnetic PCH (20% Fe)	25	20

Ethylene Adsorption

Adsorption behavior of ethylene gas within the magnetic PCHs and PCH (D/T=20/200) materials was examined using gas chromatography. The magnetic PCHs and PCH are modified for utilize as ethylene scavenger in food packaging film due to the physical characteristics of these porous clays such as surface area, pore size and also Fe ions on the surface. The samples must be heated before ethylene adsorption would occur to remove volatile molecules from the porous clays. Figure 4.11 depicts the adsorption capacity of the magnetic PCHs and PCH. The amount of ethylene adsorption proportionally increased with time. Moreover, adsorption rates for these ethylene scavenger are fast at the beginning. The capacity of magnetic PCHs prepared by the incorporation of Fe ions on the surface and in the porous structure was significantly better than PCHs due to Fe ions. From the results in this work, it was clear that the enhancement of the ferric chloride hexahydrate on PCHs play an important role in ethylene adsorption. So it was possible to use these porous clays and Fe ions as ethylene scavenger.

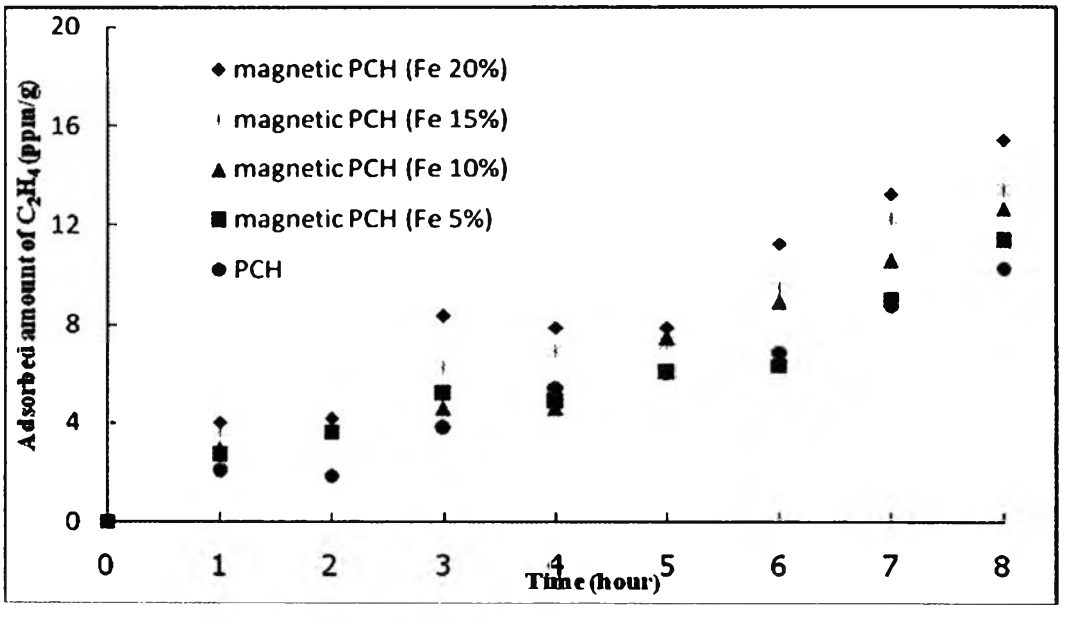

Figure 4.11 Ethylene adsorption capacity of magnetic PCHs and PCH.

4.5 Conclusions

Porous clay heterostructures (PCHs) derived from Na-bentonite clay has been synthesized by a surfactant directed assembly of silica species within the clay galleries. From the analysis of N_2 adsorption-desorption data, the results showed that PCHs and magnetic PCHs had surface areas of 412–688 m^2/g and 148–170 m^2/g, respectively. The isotherms of PCHs and magnetic PCHs belong to type IV, corresponding to mesoporous adsorbents. When bentonite was treated with CTAB, the distance between clay layers increased as investigated by XRD. There was no obvious peak observed in the XRD patterns of magnetic PCHs due to the disordered structure of silica framework. SEM images, EDX micrographs and UV adsorption of magnetic PCHs showed incorporation of Fe ion in PCH is successful. Magnetic PCH exhibited a remarkably significant bacteriostatic effect against *Escherichia coli* and *Staphylococcus aureus*.

4.6 Acknowledgements

This work is funded by National Research Council of Thailand (NRCT). The authors would also thanks Polymer Processing and Polymer Nanomaterial Research Unit and the Center of Excellence for Petroleum, Petrochemical, and Advanced Materials, Thailand for their partially funding.

4.7 REFERENCES

[1] Galarneau, A., Barodawalla, A., and Pinnavaia, T.J. Nature 374 (1995) 529.

[2] Pires, J., Araujo, A.C., Carvalho, A.P., Pinto, M.L., Gonzalez-Calbet, J.M., and Ramirez-Castellanos, J. Micropor. Mesopor. Mater. 73 (2004) 175.

[3] Polverejan, M., Pauly, T.R., and Pinnavaia, T.J. Chem. Mater. 12 (2000) 2698.

[4] Pichowicz, M., and Mokaya, R. Chem. Commun. (2001) 2100.

[5] Galaneau, A., Barodawalla, A., and Pinnavaia, T.J. Chem. Commun. (1997) 1661.

[6] Polverejan, M., Liu, Y., and Pinnavaia, T.J. Chem. Mater. 14 (2002) 2283.

[7] Zhu, H.Y., Ding, Z., and Barry, J.C. J. Phys.Chem. B. 106 (2002) 11420.

[8] Prakobna, K., Luangsukrerk, S., Magaraphan, R., and Manuspiya, H. Nano/Micro Engineered and Molecular Systems. 16(2007) 483.

[9] Srithammaraj, K., Magaraphan, R., and Manuspiya, H. Advance Materials Research. 55(2008), 317.